

Effect of Interstitial Content on High-Temperature Fatigue Crack Propagation and Low-Cycle Fatigue of Alloy 720

S. Bashir and M.C. Thomas

Alloy 720 is a high-strength cast and wrought turbine disc alloy currently in use for temperatures up to about 650 °C in Allison's T800, T406, GMA 2100, and GMA 3007 engines. In the original composition intended for use as turbine blades, large carbide and boride stringers formed and acted as preferred crack initiators. Stringering was attributed to relatively higher boron and carbon levels. These interstitials are known to affect creep and ductility of superalloys, but the effects on low-cycle fatigue and fatigue crack propagation have not been studied. Recent emphasis on the total life approach in the design of turbine discs necessitates better understanding of the interactive fatigue crack propagation and low-cycle fatigue behavior at high temperatures. The objective of this study was to improve the damage tolerance of Alloy 720 by systematically modifying boron and carbon levels in the master melt, without altering the low-cycle fatigue and strength characteristics of the original composition. Improvement in strain-controlled low-cycle fatigue life was achieved by fragmenting the continuous stringers via composition modification. The fatigue crack propagation rate was reduced by a concurrent reduction of both carbon and boron levels to optimally low levels at which the frequency of brittle second phases was minimal. The changes in composition have been incorporated for production disc forgings.

Keywords

Alloy 720, fatigue crack propagation, high temperature fatigue, IN718, jet engines, low cycle fatigue, superalloys, Waspaloy IN718

1. Introduction

In aerospace applications, there is a continuous quest to reduce weight and to move to high-strength materials with greater tolerance to higher design stresses and temperatures. Materials for critical rotating parts, e.g., turbine discs, traditionally have been designed for burst margins, fatigue crack initiation, and creep strength. Since the early 1980s, regulatory evolutions by defense agencies and the Federal Aviation Administration (FAA) have put explicit demands on the total life approach to ensure sufficient damage tolerance of the newer engines.^[1] The "retirement-for-cause" approach, for instance, resulted in fatigue crack propagation (FCP) programs like ESDADTA^[2] and ENSIP.^[3]

Fatigue resistance of nickel-base superalloys is affected by grain size, gamma prime (γ') size and morphology, carbides and other phases, and by the presence of processing defects like porosity and oxide inclusions.^[4-7] Chemical composition, material processing, and heat treatment may be altered to design a microstructure to derive desired properties. Composition control is the first step in this process. It is important to realize that major changes in microstructure and properties can be caused by relatively small changes in composition. Improved under-

standing of microstructure effects on creep and low-cycle fatigue (LCF) of superalloys contrasts a similar systematic understanding of FCP behavior. Understanding of FCP behavior becomes even more important, considering the increasingly extreme operating conditions encountered in modern jet engines.

Alloy 720 is a high-strength cast and wrought turbine disc alloy currently in use for temperatures up to about 650 °C in Allison's T800, T406, GMA 2100, and GMA 3007 engines. In the original composition intended for use as turbine blades (Table 1), the carbon and boron levels resulted in carbide and boride stringers that acted as preferred fatigue crack initiation sites. These deliberately added interstitial elements are known to significantly alter creep and ductility of superalloys.^[8,9] However, the effects of these elements on FCP and LCF have not been studied. The objective of this study was to improve the damage tolerance of Alloy 720 by systematically modifying carbon and boron levels in the master melt, without altering the LCF and strength characteristics of the original composition.

2. Materials

Two experimental heats (300 lb each) were vacuum induction melted/vacuum arc remelted (VIM-VAR) melted, homogenized, and finish rolled to produce a uniform grain size of ASTM No. 10 to 12, by the Special Metals Corporation, New Hartford, N.Y. These represent the two modified compositions, Conditions A and B. For the baseline, disc forgings with identical grain sizes were used. The compositions are given in Table 1. All specimen blanks were then identically heat treated as follows: 1100 °C, 2 h, OQ; 760 °C, 8 h, AC; 650 °C, 24 h, AC.

S. Bashir, Systems Engineering, GMA 3007 Engine Program, and M.C. Thomas, Materials and Processes Engineering, Allison Gas Turbine Division, General Motors Corporation, Indianapolis, Indiana 46206.

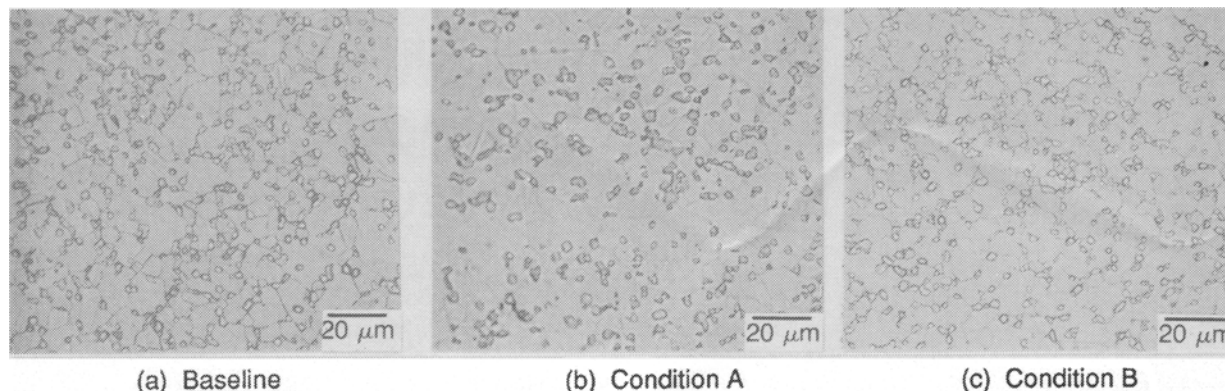


Fig. 1 Optical micrographs of fully heat treated microstructures.

Table 1 Alloy compositions used in study

	C	B	Zr	Ti	Composition, wt%		Mo	Co	W	Ni
					Al	Cr				
Baseline	0.03-0.04	0.03-0.04	0.025-0.050	4.75-5.25	2.25-2.75	17.5-18.5	2.75-3.25	14.0-15.5	1.10-1.40	Bal
Condition A....	0.012	0.017	0.029	4.93	2.54	17.01	3.02	14.52	1.22	Bal
Condition B....	0.011	0.029	0.030	4.95	2.55	17.14	3.03	14.54	1.22	Bal

3. Experimental Procedure

3.1 Metallography

Cross sections for optical and scanning electron microscopy (SEM) metallography were polished to 1 μm finish and analyzed in the as-polished condition for stringers and other phases. These were then electropolished and immersion etched using a procedure developed by Radavich.^[10] The SEM analysis was conducted in the electropolished and also in the electropolished and etched condition, and SEM fractography was conducted on FCP and LCF specimens.

3.2 Mechanical Testing

Tensile tests at room temperature and 650 $^{\circ}\text{C}$ were conducted on 1.27 cm (0.5 in.) diam standard specimens per ASTM Standard E8. Smooth bar longitudinal strain-controlled LCF tests were conducted on a computer-controlled servohydraulic system at 427 $^{\circ}\text{C}$, $R = 0.0$, at 20 cpm using triangular waveform. Compact tension specimens 3.90W \times 0.63 cm (1.5W \times 0.25 in.) thick were used for fatigue crack propagation tests conducted per ASTM Standard E647 at 650 $^{\circ}\text{C}$, $R = 0.05$ at 200 cpm. The crack extension was measured by a traveling microscope.

4. Results and Discussion

4.1 Microstructure

For the three conditions studied, the microstructures are shown in Fig. 1. The grain size was identically uniform and averaged ASTM No. 10 to 12. Fine γ' averaged about 0.1 to 0.2 μm . Due to the fineness of the microstructure, high magnifica-

tions were needed in both optical and SEM metallography. The baseline microstructure consisted of boride and carbide stringers ranging in size from 100 to 500 μm (Fig. 2a). Radavich^[10] and Liu^[11] have reported that the phases present in Alloy 720 are Mo- and Cr-rich M_3B_2 or MB_2 borides, Ti-rich blocky MC carbides, M_{23}C_6 carbides, and occasional TiCN. Compared to the baseline, Condition B, in which carbon is 0.011% and boron is identical, stringers were fewer and smaller, ranging from 25 to 125 μm (Fig. 2b). Mostly, these were borides. For Condition A with the lowest boron and carbon levels, the stringers were absent, and the second phases were dispersed and finer.

4.2 Effects of Boron and Carbon

This section discusses the roles by which the controlled trace elements boron and carbon benefit nickel-base superalloys. Both are added in the melt and have been reported to affect microstructure and properties of superalloys, stainless steels, and intermetallic compounds.^[12-15] Boron was originally added as a fluxing agent, and in the late 1950s, trace amounts of boron in melts improved hot workability and creep-rupture properties of various steels.^[16] The amount required for property enhancement was very low. In Waspaloy, only 15 ppm of boron was sufficient to double the stress-rupture life.^[9] These improvements were attributed to stabilization of grain boundaries and phases present as a result of boron segregation to the boundaries. The segregation of boron is believed to (1) increase grain boundary cohesion, (2) reduce grain boundary surface energy, (3) lower grain boundary diffusion rates, and (4) change γ , γ' , and/or M_{23}C_6 morphologies. It also lowers the solidus temperature.^[14,17,18]

The solubility of boron in nickel is limited, and above the limit, it forms complex Mo- and Cr-rich boride clusters and stringers, as discussed above. The continuous stringers are mi-

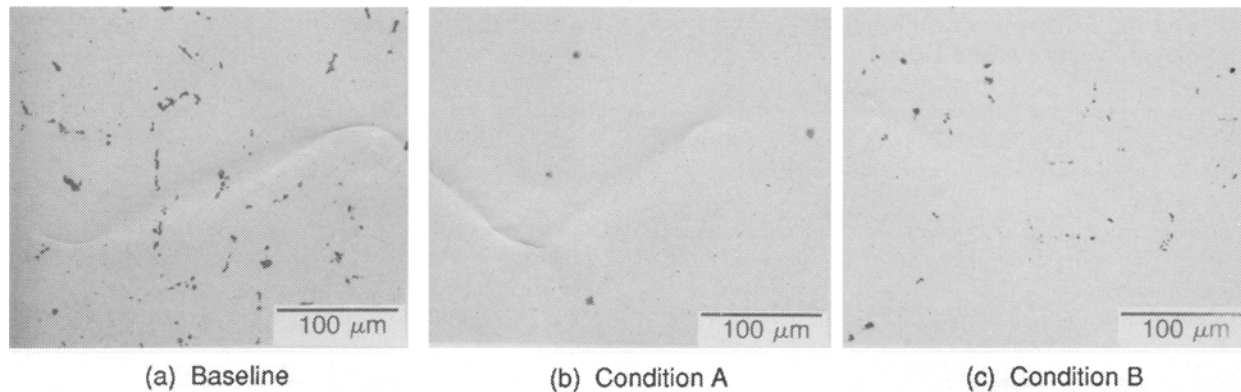


Fig. 2 As-polished optical micrographs. (a) Large stringers. (b) Absence of continuous inclusions. (c) Stringers broken into smaller lengths and individual particles.

Table 2 Average monotonic tensile properties

	Ultimate tensile strength, MPa	0.2% yield strength, MPa	Elongation, %	Reduction of area, %
At 24 °C				
Baseline	1675.3	1282.3	15.0	17
Condition A	1661.5	1261.6	16.5	18.7
Condition B	1682.2	1275.4	18.4	20
At 650 °C				
Baseline	1468.5	1199.6	12.3	15.2
Condition A	1447.7	1178.9	12.8	15.5
Condition B	1427.0	1185.8	9.0	10.2

crostructural inhomogeneities that act as preferred crack initiators detrimental to LCF life. One way to eliminate the continuity and minimize the presence of stable, brittle borides is to reduce boron to below the solubility limit for a given material. This was achieved in the present study by systematically altering boron from 0.04 to 0.017%. The effects of this change in boron content on LCF and FCP are discussed in a later section.

In superalloys, carbon is added as a refiner during melting and generally results in the formation of MC, M_7C_3 and $M_{23}C_6$ carbides, and TiCN.^[19] Noncontinuous intergranular carbides improve creep resistance by grain boundary pinning, whereas continuous carbides are known to act as crack initiators and also degrade stress-rupture properties.^[20] As expected, both MC and $M_{23}C_6$ carbides were present in the microstructures studied. Relative to the baseline, the frequency of carbide clusters and also of discrete blocky carbides was less in Conditions A and B.

Similar to boron, the presence of carbon above a certain limit leads to formation of continuous carbides. In an earlier work on Waspaloy,^[21] 0.045% carbon produced carbide clusters and stringers quite similar to the present baseline condition. Reduction of carbon to 0.01 to 0.02% eliminated stringers without any degradation in strength or ductility. Recently, it was reported that extra-low carbon (about 0.01%) in IN-718 reduced the tendency of stringer formation and improved the LCF life.^[21] However, there is evidence that too low a carbon level in superalloys reduces creep properties.^[22]

Because a certain minimum amount of carbon is needed in superalloys for melt refining as well as carbide formation, it follows that an optimally low level of carbon is desirable. The present study has shown that to be at least 0.01% for Alloy 720.

5. Mechanical Properties

5.1 Tensile Properties

Average monotonic tensile data for the three conditions are summarized in Table 2. The tensile properties are identical at all temperatures.

5.2 Low-Cycle Fatigue

The strain-controlled low-cycle fatigue data for the three conditions are compared in Fig. 3. In the baseline condition, a majority of the cracks that initiated at the surface or near the surface were boride or carbide stringers. Figure 4 is characteristic of such an origin. As described earlier, the stringer length varied from 100 to 500 μm . There is evidence that the LCF life is related to the size of microstructural defects in superalloys.^[23-25] The probabilistic distribution and location of such defects increases the scatter of LCF life, and they are relatively more detrimental when they are surface related.^[26,27] Tests were specifically conducted to investigate this behavior for the baseline condition. The conditions for the smooth bar

LCF tests were 0-0.87%-0 total strain at 426 °C and 20 cpm. The life versus stringer size data from these tests (Fig. 5) reveal a noticeable scatter in life. Similar tests conducted on material with lower carbon levels of 0.025 and 0.019% (at constant boron) exhibited less scatter and a gradual transition in initiation from surface-related stringers to primarily crystallographic initiation.

Because the grain size, γ' size and major chemical elements, and the processing and heat treatment are identical for the three conditions, improvement in LCF life is the result of the redistribution of phases due to small changes in the carbon and boron levels.

5.3 Fatigue Crack Propagation

From the da/dN versus ΔK plot at 650 °C (Fig. 6), the FCP resistance of Condition B relative to the baseline composition improved by a factor of 3 when carbon was lowered and boron was constant (at $\Delta K = 22 \text{ MPa} \sqrt{\text{m}}$). The dominant crack propagation mode was intergranular (Fig. 7) as would be expected for such a fine grain structure. The cracks appeared to follow

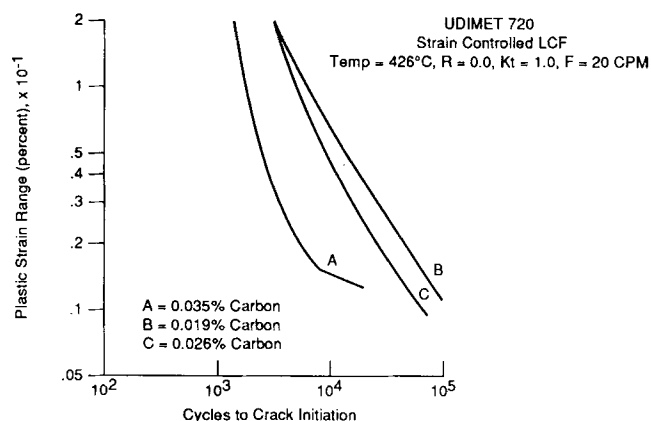


Fig. 3 Strain-controlled LCF data reveal the effect of carbon levels.

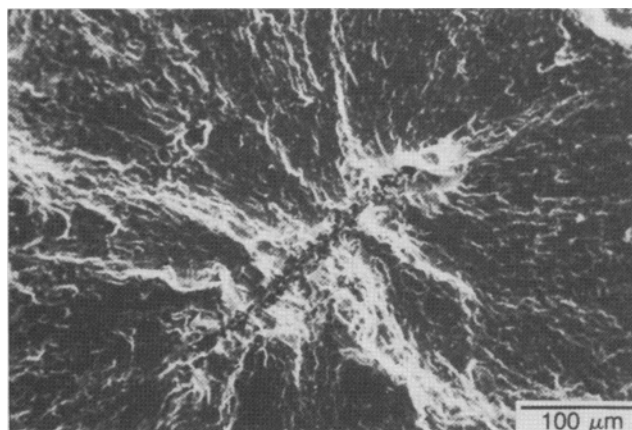


Fig. 4 Characteristic LCF crack initiation in the baseline composition at a near-surface boride for a test at $\Delta\epsilon_f = 0.87\%$, $T = 426^\circ\text{C}$, $K_t = 1.0$.

the continuous stringers in the baseline condition (Fig. 8) and also were observed originating at cracked MC carbides (Fig. 9). The improved resistance to crack growth in Condition B is due to fewer brittle stringers and blocky carbides, which if readily available as in the baseline condition, provide less accommodation for crack tip plasticity.

A further improvement by 2.5 \times in the FCP resistance is achieved by lowering the boron level (at constant carbon), as shown in Fig. 6. The crack propagation mode was similar to the other two conditions at this stress intensity. As described earlier, lower carbon and boron levels formed smaller dispersed

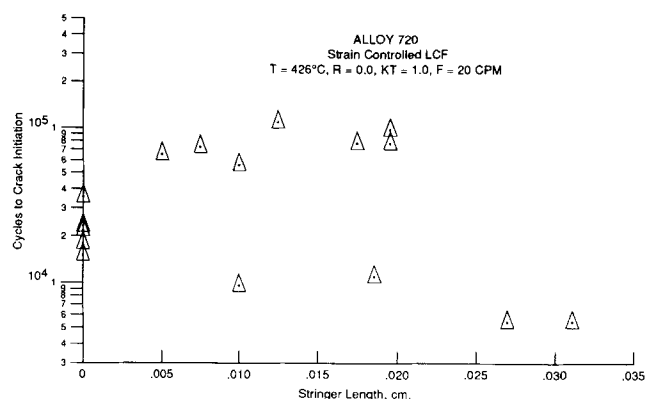


Fig. 5 Stringer size effect on strain-controlled LCF life in the baseline composition at constant $\Delta\epsilon_f = 0.87\%$, $T = 426^\circ\text{C}$, $K_t = 1.0$.

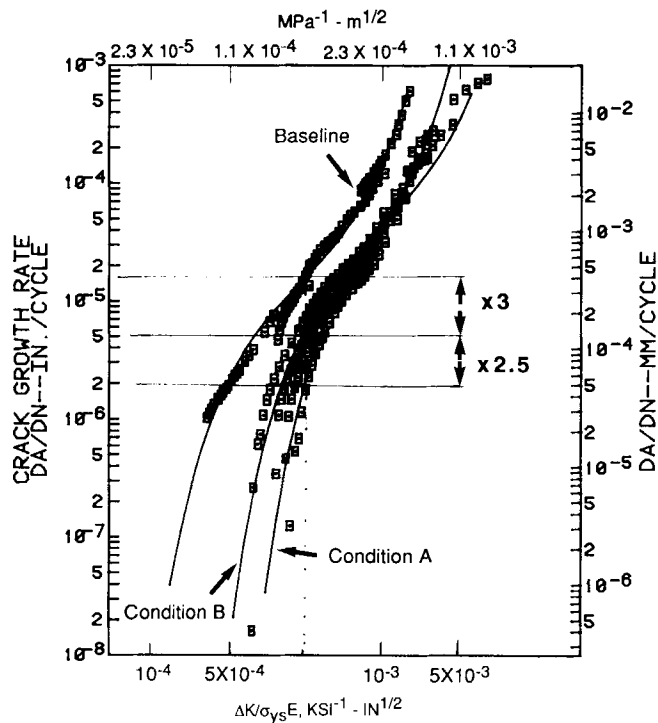


Fig. 6 Fatigue crack growth rate normalized with yield strength and modulus at 650 °C, $R = 0.05$, $F = 200$ cpm.

second phase particles compared to the large continuous stringers in the baseline condition. Smaller particles in Condition A tend to deflect the crack front, thus improving the resistance to crack advance.

At very high temperatures (i.e., 650 °C), intergranular crack propagation in fine-grained turbine disc alloys has been largely attributed to environmental embrittlement of grain boundaries, although the exact mechanism is still being debated. Some of the proposed modifications for improving FCP resistance of superalloys include changes in grain size, γ' size, strength, and

composition. However, it is known that improvements in FCP generally affect the competing LCF and creep behavior. In the present study, only composition was modified whereas all other variables were kept constant.

The present work on Alloy 720 clearly identifies a practical solution for improving FCP resistance without altering LCF. Carefully controlled amounts of the interstitial elements boron and carbon in the melt have concurrent benefits of improving the FCP resistance without affecting other properties. Of particular importance is the fact that these improvements have been achieved without requiring changes to the heat treatment or the fabrication process. Similar significant improvements may be obtained in other turbine disc alloys by the relatively inexpensive and simple method of controlling minor elements in the melt.

6. Conclusions

Trace elements can significantly alter the microstructure and mechanical behavior of superalloys. Improvements in high-temperature fatigue crack propagation are possible without altering the low-cycle fatigue properties. Boron and carbon are beneficial to superalloys in carefully controlled trace quantities. Excessive amounts result in microstructural inhomogeneities, whereas too low amounts could degrade creep capability and producibility.

A much greater emphasis on understanding fatigue crack propagation is needed in the design of turbine disc alloys. Development and improvement in advanced materials require a multifaceted approach. Composition, processing, and microstructure are equal contributors to the mechanical behavior and must be understood in systematic fundamental ways. Without this, the full capabilities of materials will never be achieved.

Acknowledgments

The authors wish to thank Allison Gas Turbine, Division of General Motors Corporation, for funding this work. They ac-

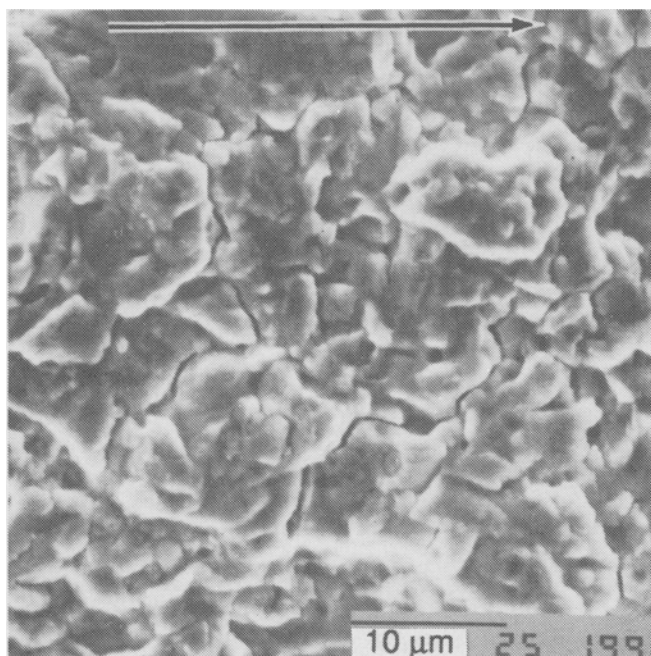
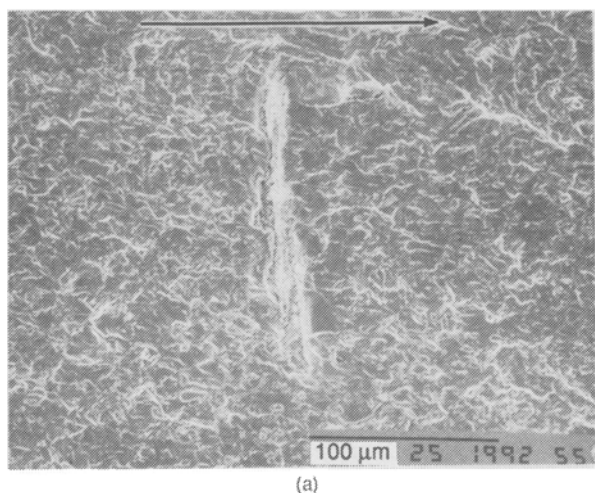
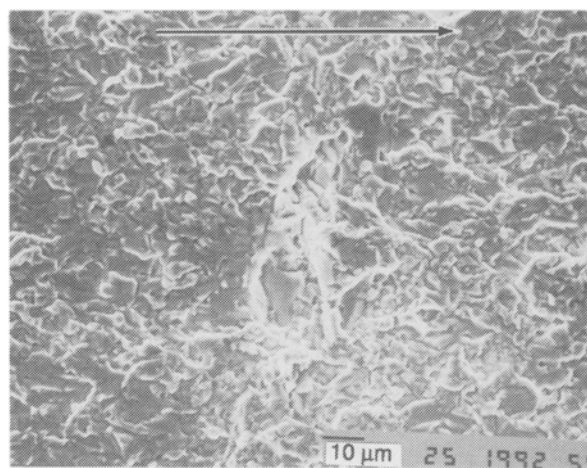


Fig. 7 Intergranular cracking is the dominant crack propagation mode in all three conditions. Fractograph is from a test in Condition B.



(a)



(b)

Fig. 8 Fractograph from a FCP test in the baseline composition. (a) Mo-rich boride. (b) Ti-rich carbide.

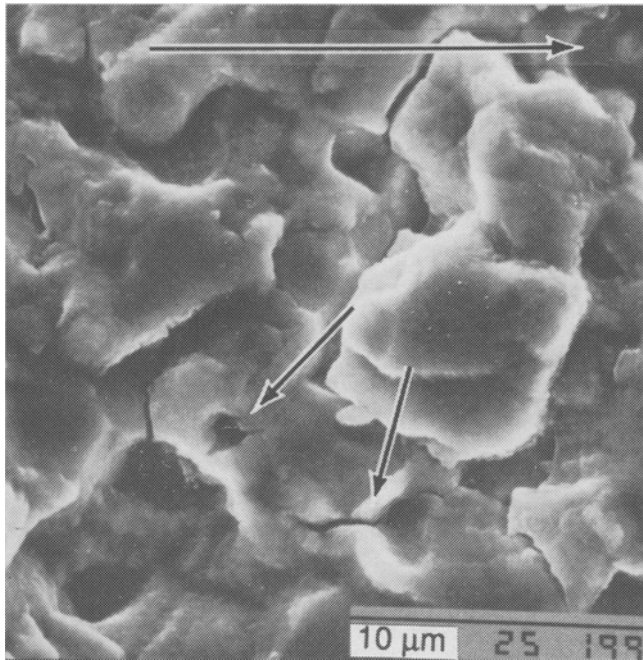


Fig. 9 Cracks observed at carbides. Fractograph is from a FCP test in Condition B.

knowledge Special Metals Corporation for supplying the material and also acknowledge M. Khan for testing and Ms. Marsha Gray for compiling the data.

References

1. R.H. Jeal, AGARD Report No. 769, 1988, p 1.1-1.7
2. ESDADTA Phase II Report, U.S. Navy Contract N 00019-85-C-0034, Sept 1980
3. ASIP/ENSIP Conf. Proc., AFWAL-TR-88-4128, U.S. Air Force, Dayton, June 1988
4. J. Gayda, R.V. Miner, and T.P. Gabb, *Superalloys 1984*, M. Gell et al., Ed., Met. Soc. AIME, 1984, p 731-739
5. S.D. Antolovich and N. Jayaraman, *Fatigue*, J.J. Burke and V. Weiss, Ed., Plenum Press, 1983, p 119-144
6. S. Bashir and S.D. Antolovich, *Superalloys 1984*, M. Gell et al., Ed., Met. Soc. AIME, 1984, p 295-307
7. G.L.R. Durber, C.L. Jones, and A.J. Dykes, *Superalloys 1984*, M. Gell et al., Ed., Met. Soc. AIME, 1984, p 433-442
8. C.G. Bieber and R.F. Decker, *Trans. AIME*, Vol 221, 1961, p 629
9. F.N. Darmara, *J. Iron Steel Inst.*, Vol 191, 1959, p 268
10. J.F. Radavich, Seminar on Alloy 720, Purdue University, July 1990
11. L. Liu, M.S. thesis, Purdue University, 1990
12. R.F. Decker and J.W. Freeman, *Trans. AIME*, Vol 218, 1961, p 277
13. W.J. Pennington, *Met. Prog.*, Vol 73, 1958, p 82
14. T.J. Garosshen, T.D. Tillman, and G.P. McCarthy, *Metall. Trans. A*, Vol 18, Jan 1987, p 69-77
15. T.H. Chuang, Y.C. Pan, and S.E. Hsu, *Metall. Trans. A*, Vol 22, Aug 1991, p 1801-1809
16. R.F. Decker, *High Temperature Materials*, R.F. Hehemann and G.M. Ault, Ed., John Wiley & Sons, 1959, p 388
17. C.L. White, J.H. Schneibel, and R.A. Padgett, *Metall. Trans. A*, Vol 14, Apr 1983, p 595-610
18. M. McLean and A. Strang, *Met. Tech.*, Vol 14, Oct 1954, p 454
19. C.T. Sims, N.S. Stoloff, and W.C. Hagel, Ed., *Superalloys II*, John Wiley & Sons, 1987
20. T.J. Garosshen and G.P. McCarthy, *Metall. Trans. A*, Vol 16, July 1985, p 1213-1223
21. J.J. Moyer, *Superalloys 1984*, M. Gell et al., Ed., Met. Soc. AIME, 1984, p 443-454
22. J.P. Stroup and L.A. Pugliese, *Met. Prog.*, Vol 93, Feb 1968, p 96-100
23. S. Bashir, Ph.D. dissertation, University of Cincinnati, 1982
24. J. Hyzak and I.M. Bernstein, *Metall. Trans. A*, Vol 13, Jan 1982, p 33-43
25. J. Hyzak and I.M. Bernstein, *Metall. Trans. A*, Vol 13, Jan 1982, p 45-52
26. A. Pineau, *High Temperature Materials for Power Engineering*, E. Bachelet et al., Ed., Kluwer Academics, 1990, p 913-934
27. C.E. Shambley and D.R. Chang, *Metall. Trans. A*, Vol 16, 1985, p 775-784